Auralisation of accelerating passenger cars

Reto Pieren, Thomas Bütler, Kurt Heutschi
Empa, Swiss Federal Laboratories for Materials Science and Technology, Duebendorf, Switzerland.

Summary
Within the research project TAURA, a traffic noise auralisator will be developed that covers road traffic and railway noise. The key element is a synthesiser that simulates the acoustical emission of a great many of different vehicles, operating on a wide variety of surfaces and under different operating conditions. To obtain the corresponding steering parameters, a hierarchic synthesiser structure with core parameters and global parameters is proposed. While the core parameters will be determined with controlled experiments for a small number of vehicles, the global parameters are measured for a large vehicle fleet. This paper focusses on the emission synthesiser of accelerating passenger cars. The core parameters for the tyre noise sources were determined from coast-by measurements of passenger cars with idling engine. To obtain the propulsion noise parameters, measurements at different engine speeds, engine loads and emission angles were performed using a chassis dynamometer. The structure of the additive sound synthesiser and the signal processing algorithms to extract its steering parameters from measurement data will be presented.

PACS no. 43.50.Lj, 43.50.Rq, 43.58.Jq, 43.60.Cg

1. Introduction

Very recently, auralisation has been discovered for outdoor noise applications. Within the Swedish project LISTEN [1][2] and the European project HOSANNA [3], tools for the auralisation of traffic noise were developed. The main motivation is to provide more intuitive information about traffic noise scenarios for city planners, noise consultants and decision makers. There is common agreement in the point that information about noise in form of dB values is difficult to communicate to the public [4] and that the quality of noise mitigation measures shifts to perceptual efficiency [5].

2. Model

The model to auralise accelerating passenger cars comprises an emission, a propagation and a reproduction module. Fig. 1 shows the flow chart of the model. The input parameters describe the vehicle, the driver, the road, the geometry, the ground type and the weather—the input parameters marked by * are time dependent. The left half of Fig. 1 represents the emission module in which the emitted sounds are synthesised. Consequently, for each source signal a propagation filtering is applied. Finally, the contributions of all sources are rendered for multi-channel reproduction and summed up.

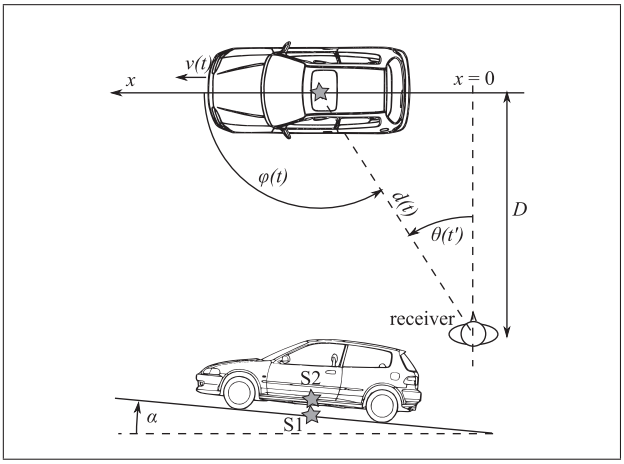

Figure 2. Sketch of the geometrical situation.

The emission model describes the emitted sound of an individual passenger car pass-by, i.e. its outside sound. It consists of an additive synthesiser whose parameters are obtained from controlled measurements. In order to have a defined interface to the sound propagation filtering, a point source model is adopted with each point source having emission angle dependent signal characteristics.

The acoustical emission of the passenger car is assumed to consist of the two contributions tyre/road sound and propulsion sound. For a given road and car, the tyre sound source signals s_{tyre} are assumed

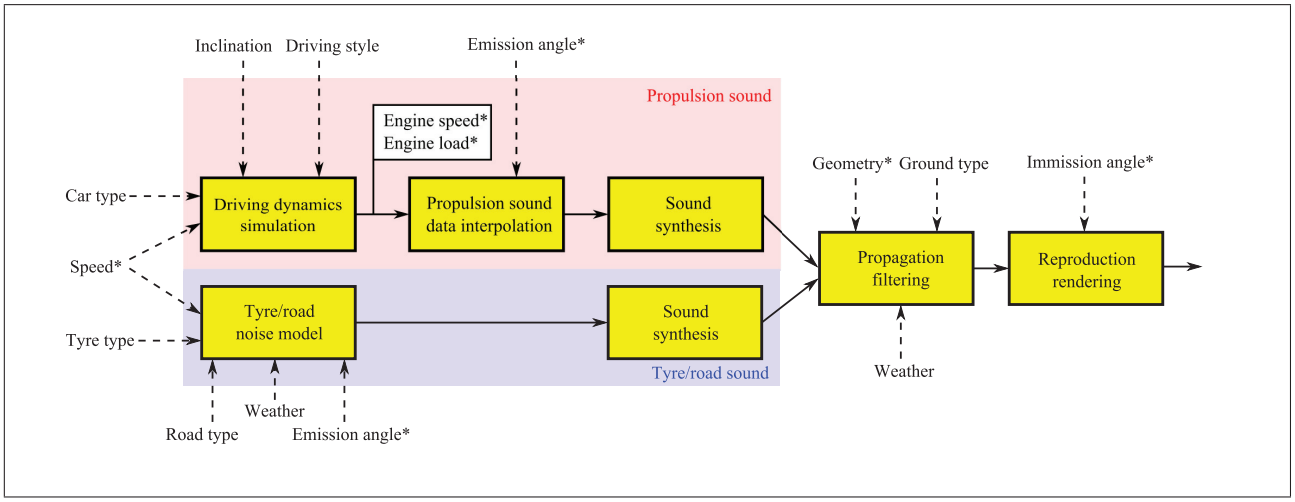

Figure 1. Simulation flow chart of the auralisation of accelerating passenger cars. The input variables marked by a * are time-dependent.

to depend on the speed v and the emission angle φ. Whereas the propulsion sound source signal s_{prop} is assumed to depend on the engine speed n, the engine load Γ and the emission angle φ. As input parameter describing the kinematics of the vehicle, its speed $v(t)$ in km/h along the x-axis as function of time t (at the source) is used throughout this paper. The geometrical situation is depicted in Fig. 2 in which the distance of the driving lane to the receiver is D , the immission angle is θ, the angle of inclination α and the point source positions S1 and S2, respectively. In correspondence with the Harmonoise model [6], the point sources $S1$ and $S2$ are vertically stacked and located at heights 0.01 and 0.3 m above ground. The propulsion sound signal is fully attributed to the upper point source. However, the sound powers of the tyre sound contribution are distributed over the point sources by 80/20 % [6].

2.1. Driving dynamics

The engine speed n in engaged mode reads

$$n(t) = 60 \cdot i_{\mathrm{gear}} \cdot i_{\mathrm{ax}} \cdot \frac{v(t)/3.6}{2\pi r_{\mathrm{tyre,dyn}}} \quad [\mathrm{rpm}] \qquad (1)$$

with the gear ratio i_{gear}, the axle ratio i_{ax} and the dynamic tyre radius $r_{\mathrm{tyre,dyn}} \approx 0.3$ m. The traction F_T is modelled by

$$F_{\mathrm{T}}(t) = F_B(t) + \bar{e}m \cdot a(t) + mg\sin(\alpha) \quad [\mathrm{N}] \qquad (2)$$

$$F_B(t) = F_1 + F_2 \cdot v(t) + F_3 \cdot v^2(t) \qquad (3)$$

$$a(t) = \frac{dv(t)/3.6}{dt} \qquad (4)$$

with the vehicle mass m, gravity g, the translational acceleration a of the car and a mean equivalent mass factor $\bar{e} = 1.15$ for the rotational accelerations. The

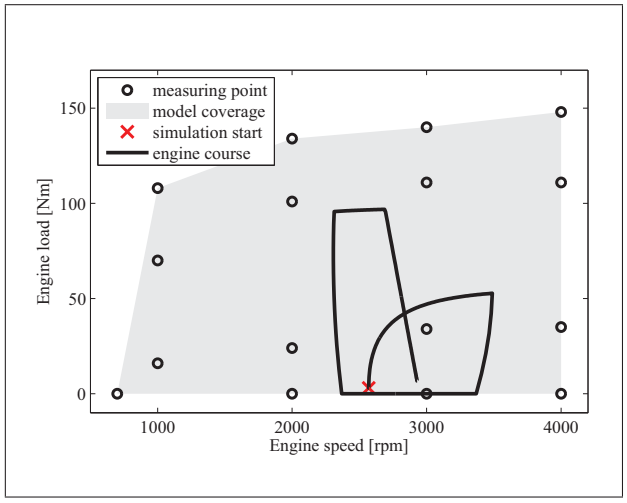

Figure 3. Simulated engine condition course of an accelerating Ford Focus 1.8i within the model coverage region (grey) spanned by the measuring points (circles). The topmost circles at 1000 to 4000 rpm are at full load.

basic driving resistance F_B (consisting of rolling resistance and aerodynamic drag) is modelled by the coast-down parameters F_1, F_2 and F_3 with units N, N/(km/h) and N/(km/h)^2 respectively. The engine load (torque) is formulated by

$$M(t) = \frac{r_{\mathrm{tyre,dyn}} \cdot F_{\mathrm{T}}(t)}{\eta \cdot i_{\mathrm{gear}} \cdot i_{\mathrm{ax}}} \quad [\mathrm{Nm}] \qquad (5)$$

with a globally set efficiency factor $\eta = 0.9$ for the power transmission from the engine to the wheels. The engine load in percent is defined by

$$\Gamma(t) = \frac{M(t)}{M_{\max}(n(t))} \cdot 100 \quad [\%] \qquad (6)$$

Fig. 3 shows an engine condition course which was simulated with the described model. The car accelerates from 20 km/h to 40 km/h. At 3500 rpm the

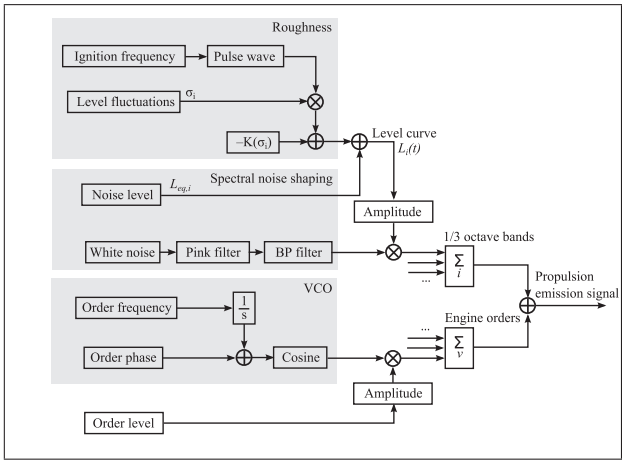

Figure 4. Flow chart of the propulsion sound synthesiser.

gearbox is shifted from first to second gear, i.e. the clutch is disengaged, the second gear is put in (at idling engine) and the clutch is engaged again.

2.2. Emission synthesiser

The structure of the emission synthesiser is similar to the one recently published for wind turbine sounds [7]. The emission signal of the tyre sound component is assumed to consist of broadband noise only, i.e. discrete tones due to e.g. tyre tread resonances or discrete vibrational tyre resonances are not taken into account. The spectral shaping of the broadband noise components is performed in 1/3 octave bands. The sound pressure emission signals of the tyre sound component are calculated by

$$s_{\mathrm{tyre}}(t) = \sum_{i=1}^{N_b} p_0 10^{L_{\mathrm{tyre},i}(v(t),\varphi(t))/20} \cdot n_i(t) \qquad (7)$$

with N_b being the number of considered 1/3 octave bands, the reference pressure $p_0 = 20$ μPa and normalized bandpass filtered noise signals $n_i(t)$. For the sound pressure level $L_{\mathrm{tyre},i}$ of band i a common logarithmic speed relationship is assumed

$$L_{\mathrm{tyre},i}(t) = A_i + B_i \cdot \log\left(\frac{v(t)}{v_0}\right) + \Delta L_{\mathrm{road}} + \Delta L_{i,\mathrm{dir}}(\varphi(t)) \qquad (8)$$

with reference speed $v_0 = 70$ km/h, regression parameters A_i and B_i, the road surface correction ΔL_{road} and a horizontal directivity $\Delta L_{i,\mathrm{dir}}$ for the lower source position (S1) simulating the horn effect.

The structure of the propulsion sound emission synthesiser is depicted in Fig. 4. The sound pressure emission signal of the propulsion sound component is assumed to be the sum of a deterministic signal representing the most important engine orders and a quasi-stochastic signal:

$$s_{\mathrm{prop}}(t) = s_{\mathrm{prop,ord}}(t) + s_{\mathrm{prop,noise}}(t) \qquad (9)$$

The engine order signal is composed of the sum of the engine orders ν

$$s_{\mathrm{prop,ord}}(t) = \sum_{\nu} p_0 10^{L^{\dagger}_{\mathrm{prop,ord},\nu}(t)/20} \cdot \sqrt{2}\cos(\beta_\nu(t)) \qquad (10)$$

with the order level $L^{\dagger}_{\mathrm{prop,ord},\nu}$ and the instantaneous order phase

$$\beta_\nu(t) = \phi^{\dagger}_\nu(t) + 2\pi \int_{-\infty}^{t} F_\nu(\tau)d\tau \qquad (11)$$

with the order phase $\phi^{\dagger}_\nu$ and the order frequency

$$F_\nu(t) = \nu \cdot n(t)/60. \qquad (12)$$

Listening tests revealed that in this application the order phase is a relevant synthesiser parameter. For a four-stroke engine with N_{cyl} cylinders, the ignition frequency

$$F_{\mathrm{ign}}(t) = N_{\mathrm{cyl}}/2 \cdot n(t)/60 \qquad (13)$$

and thus the engine order corresponding to the ignition—and mostly the predominant order—is $\nu_{\mathrm{ign}} = N_{\mathrm{cyl}}/2$.

The noise signal component of the propulsion sound is modelled by

$$s_{\mathrm{prop,noise}}(t) = \sum_{i=1}^{N_b} p_0 10^{L_{\mathrm{prop,noise},i}(t)/20} \cdot n'_i(t) \qquad (14)$$

with the 1/3 octave band level

$$L_{\mathrm{prop,noise},i}(t) = L^{\dagger}_{\mathrm{eq,noise},i} + \sigma^{\dagger}_i \cdot R(t) - K(\sigma^{\dagger}_i) \qquad (15)$$

with the level $L^{\dagger}_{\mathrm{eq,noise},i}$ and a level standard deviation $\sigma^{\dagger}_i$ and a level fluctuation function $R(t)$ with zero mean and unit power. The constant K ensures that despite the level fluctuations, the Leq is not altered. This level modulation simulates the rattling sound component that elicits a roughness sensation which is particularly characteristic for low engine speeds and Diesel engines. Motivated by measurement data that showed the strongest level fluctuations at the ignition frequency, R is modelled by a quasiperiodic function with period $1/F_{\mathrm{ign}}(t)$.

The above given propulsion sound synthesiser parameters marked by †, simultaneously depend on the engine speed n, the engine load M and the emission angle φ—and are hence time-dependent. They are calculated by a triangulation-based linear 3-D interpolation of measurement data. Measurements were taken on a discrete grid, typically $n \approx$

Figure 5. Photograph showing the lab with a passenger car on the chassis dynamometer, the airstream fan in front of the car and two microphones on the floor at the left-hand room edge (emission angles $\varphi = 60°$ and $120°$).

$\{1000, 2000, 3000, 4000\}$ rpm, $\Gamma \approx \{0, 40, 70, 100\}$ % and $\varphi = \{0, 60, 120, 180\}°$ (see measuring points in Fig. 3). The synthesiser parameters are evaluated with a temporal resolution of 20 ms and linearly interpolated to the audio sampling rate. For the interpolation of the order phase, ϕ, its cyclic behaviour has to be considered in order to avoid spurious strong phase fluctuations.

3. Signal analysis

In order to obtain the emission synthesiser parameters of the propulsion sound, calibrated audio recordings ($f_s = 44.1$ kHz) at different microphone positions and engine conditions were taken. Controlled measurements on a chassis dynamometer (see Fig. 5) and—in order to correct for room influences—at idling engine under free field conditions were performed. For the following signal analysis steps always a signal length of 4 seconds is adopted.

3.1. Resampling

The emission synthesiser uses detailed information about the engine orders. These parameters are obtained by a narrowband analysis which is described in the following section. Although during the measurements the engine speed was kept fairly constant, the instantaneous order frequencies slightly fluctuate as exemplary shown in Fig. 6. In order to better separate the engine orders from the noise, a preceding resampling of the slightly non-stationary signals is required.

To do so, the instantaneous engine speed is estimated by tracking an engine order in the spectrogram. Fig. 6 shows the spectrogram of a recording made at the rear of a car with an inline-four engine idling at 1100 rpm. The tracked double ignition frequency, corresponding to the 4th engine order, is drawn as a white

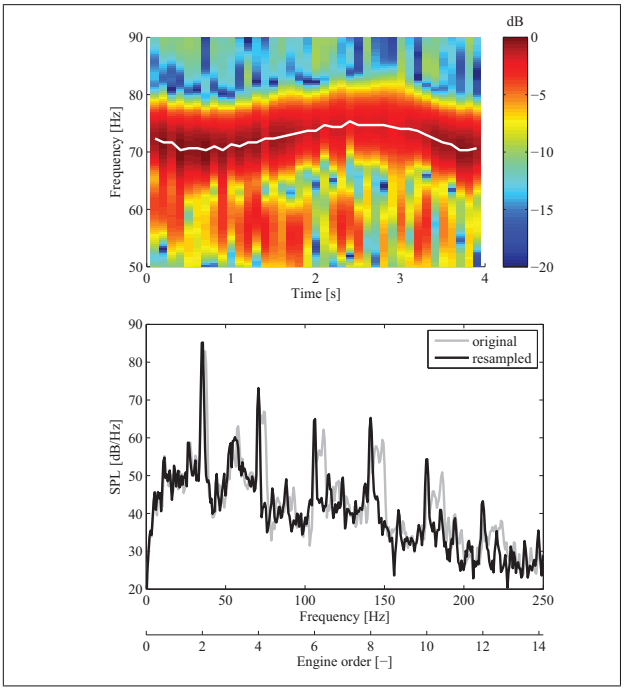

Figure 6. Normalized spectrogram of measured sound pressure signal with tracked double ignition frequency (drawn as white line) (top) and power spectral density of the original and asynchronously resampled sound pressure signal, respectively. The recording was conducted at the rear of BMW with an inline-four engine idling at 1100 rpm.

line. The lower plot illustrates the effect of the asynchronous resampling on the power spectral density. In the resampled case, all even engine orders from 2 to 12 can be clearly identified as equidistant, narrow peaks. Fig. 7 compares the effects of different resampling strategies.

3.2. Order analysis

From the resampled signals, information about the engine orders is extracted. Therefore a filter bank consisting of one bandpass filter per considered engine order is generated and applied to the signal. 8th order Butterworth filters centred around the engine order frequency F_ν with 5 Hz bandwidth are employed. At the output of each filter the corresponding order level, $L_{\mathrm{prop,ord},\nu}$ in Eq. (10), is calculated as an Leq.

The order phases are detected using the cross-correlation function. However, since the above described IIR filters introduce phase shifts, the output of each filter is time reversed and sent once again through the same filter and time reversed. In doing so, a zero-phase forward and reverse digital IIR filtering is implemented. This signal, $u_\nu(t)$, is cross-correlated with a prototype function $\cos(2\pi F_\nu t)$ to obtain the time shift

$$\kappa_\nu = \arg\max_\tau \left\{ \int u_\nu(t+\tau)\cos(2\pi F_\nu t)dt \right\} \quad (16)$$

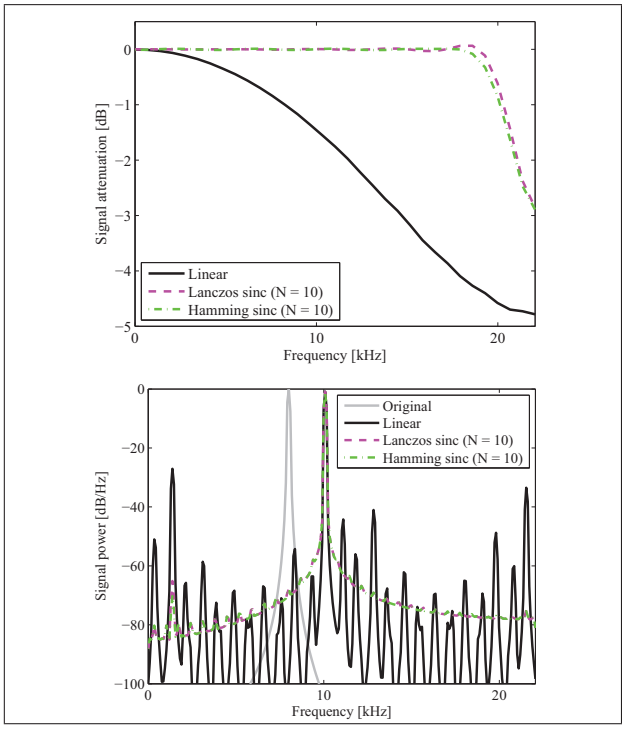

Figure 7. Spectral attenuation (top) and non-linear distortions, e.g. aliasing, (bottom) due to different resampling strategies. In the lower plot a signal containing a pure tone of 8 kHz (denoted "Original") is oversampled by a factor of $\sqrt[3]{2}$.

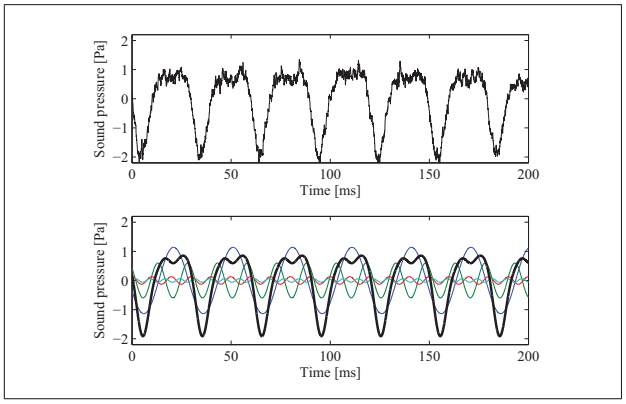

Figure 8. Comparison of sound pressure signals of a recording (top) and the corresponding synthesis consisting of engine orders with estimated phases (bottom). For the purpose of illustration only the four dominant engine orders (colored lines) are used. The recording was conducted at the rear of a Ford Focus 1.8i at 1000 rpm and full load.

from which the phase shift of Eq. (11) can be derived as

$$\phi_\nu = -2\pi F_\nu \kappa_\nu. \tag{17}$$

Fig. 8 compares the sound pressure signals of a recording and the corresponding synthesis consisting of engine orders with phases estimated by Eq. (17).

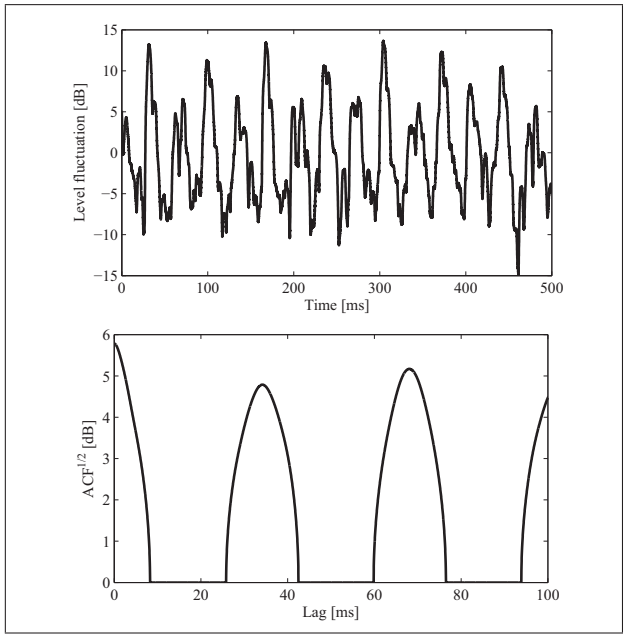

Figure 9. Level fluctuations (top) and the square root of the autocorrelation function (bottom) of the 2.5 kHz 1/3 octave band from a recording taken at the front of an idling four-cylinder Diesel engine at 870 rpm, corresponding to an ignition period of 34 ms. The lower plot indicates that the level standard deviation, σ, amounts to about 5 dB.

3.3. Noise analysis

The noise levels and their short-term level fluctuations are obtained by a series of filtering operations. Starting with the resampled signal, in a first attempt the engine orders are suppressed using cascaded notch filters. These filters are designed analogously to the engine order filter bank from the previous section except that instead of bandpass filters, band-stop filters are generated. After this operation, a 1/3 octave filter bank yields signals from which the noise levels, $L_{\mathrm{eq,noise},i}$ in Eq. (15), are calculated as Leqs. Moreover, smoothed level-time curves are calculated using a 4 ms moving average filter. Subsequently, the mean value is subtracted to obtain a DC-free level fluctuation signal, such as shown in Fig. 9. Following [7] using the autocorrelation function (ACF) of this signal, the standard deviations σ_i (used in Eq. (15)), of the level fluctuations with period $1/F_{\mathrm{ign}}$ are derived.

3.4. Backpropagation

As interface to the propagation model, the emission signals are defined at a (virtual) reference distance of 1 meter from the source position. For the measured levels L_{lab} the following inverse sound propagation model is used:

$$L_{\mathrm{Em,1\ m}} = L_{\mathrm{lab}} + 20\log\left(\frac{d_{\mathrm{Ac}}}{1\ \mathrm{m}}\right) + A_{\mathrm{room}} + A_{\mathrm{gr}} \tag{18}$$

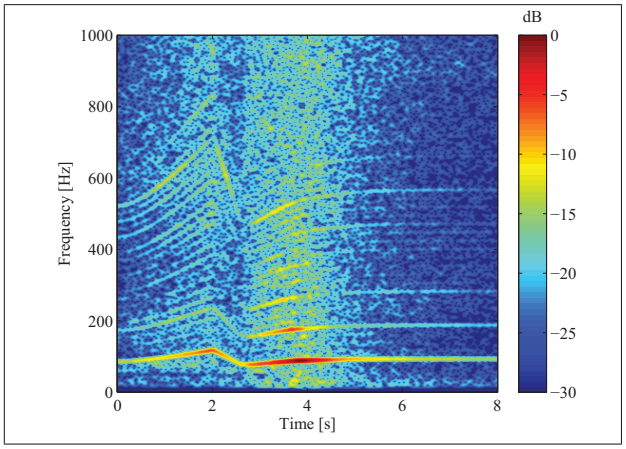

Figure 10. Spectrogram of a synthesised sound pressure signal of an accelerating passenger car pass-by (normalized to 0 dB). The engine condition course from Fig. 3 is adopted. At time 2 s the gear is shifted and at time 4 s the car passes by. As at the pass-by the engine speed still increases, the Doppler frequency shift is not directly observable in the course of the order frequencies.

with the ground effect $A_{\mathrm{gr}} = -6$ dB and A_{room} is the difference between the free field measurement and the measurement in the lab, both at idling engine ($\Gamma = 0$):

$$A_{\mathrm{room}} = L_{\mathrm{ff}}(\varphi, n, f) - L_{\mathrm{lab}}(\varphi, n, f) \tag{19}$$

d_{Ac} is the distance to the acoustical centre which, by assuming geometrical spreading of a point source, is obtained by synchronous free field measurements at two points at distances R and R' with

$$d_{\mathrm{Ac}} = \frac{R - R'}{1 - 10^{(L_{\mathrm{ff},R} - L_{\mathrm{ff},R'})/20}} \tag{20}$$

Parameters d_{Ac} and A_{room} are separately evaluated for each emission angle, engine speed and frequency band (or engine order, respectively).

4. PRELIMINARY LISTENING TESTS

A preliminary listening test was conducted with expert listeners from the disciplines acoustics and combustion engines. Auralisations of accelerating passenger car pass-bys were created by the presented model. The propagation filtering involved the Doppler and aerodynamic effects (frequency shift and amplification), geometrical spreading, air absorption and ground reflection. Fig. 10 shows a spectrogram of a synthesised audio signal which was generated by the described signal processing algorithms. At the receiver, the ORTF microphone arrangement was modelled and the resulting signals were either reproduced via a calibrated 2-channel stereo setup or headphones.

No audible artefacts such as clicks or abrupt changes were perceived—the pass-bys were considered "smooth". Generally the sound quality was assessed as "excellent". The pass-bys appeared "very plausible" and "realistic". Also the gear changes were rated as "realistic". Some listeners perceived the interferences of direct sound and ground reflection. For the playback via loudspeakers the limited reproduction of the angles of incidence (±30°) was queried. Furthermore, for conditions with dominating engine noise in the mid frequency range, the "noise component" was assessed as "too dominant". This can be attributed to the fact that in the model, tonal components which are not related to the engine speed (e.g. from fans) are reproduced by noise.

5. CONCLUSIONS

Auralisations of accelerating passenger car pass-bys generated by the presented additive synthesiser were evaluated in a preliminary listening test by expert listeners. The sound quality was assessed as excellent and the pass-bys appeared plausible and realistic. Prospectively, the auralisation model will be further validated by representative listening tests in which traffic situations will be presented and compared to recordings.

Acknowledgement

This work was supported by the Swiss National and Science Foundation SNF (# 200021-149618).

References

[1] J. Forssén, T. Kaczmarek, J. Alvarsson, P. Lundén, N. M.E.: Auralization of traffic noise within the LISTEN project - Preliminary results for passenger car pass-by. In Euronoise 2009, Eighth European Conference on Noise Control. Edinburgh, Scotland.

[2] A. Peplow, J. Forssén, P. Lundén, N. M.E.: Exterior Auralization of Traffic Noise within the LISTEN project. In Forum Acusticum 2011, European Conference on Acoustics. Aalborg, Denmark, 665–669.

[3] J. Jagla, J. Maillard, N. Martin: Sample-based engine noise synthesis using an enhanced pitch-synchronous overlap-and-add method. Journal of the Acoustical Society of America **132** (2012) 3098–3108.

[4] P. McDonald, H. Rice, S. Dobbyn: Auralisation and Dissemination of Noise Map Data Using Virtual Audio. In Euronoise 2009, 8th European Conference on Noise Control. Edinburgh, Scotland.

[5] A. Fiebig, K. Genuit: Development of a synthesis tool for soundscape design. In Euronoise 2009, 8th European Conference on Noise Control. Edinburgh, Scotland.

[6] H. G. Jonasson: Acoustical Source Modelling of Road Vehicles. Acta Acustica United with Acustica **93** (2007) 173–184.

[7] R. Pieren, K. Heutschi, M. Müller, M. Manyoky, K. Eggenschwiler: Auralization of Wind Turbine Noise: Emission Synthesis. Acta Acustica United with Acustica **100** (2014) 25–33.